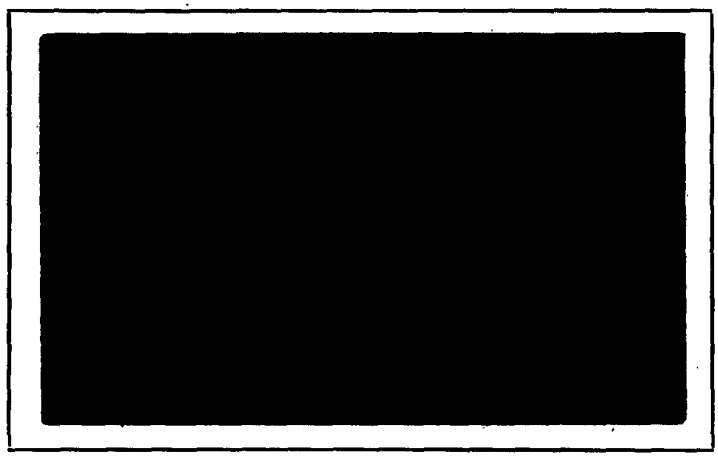

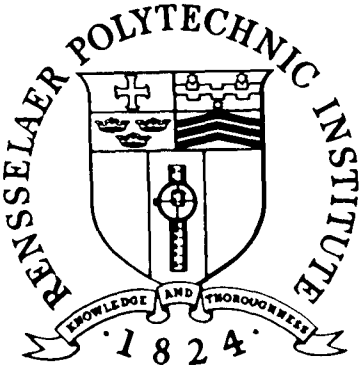

Rensselaer Polytechnic Institute

Troy, New York

RENSSELAER POLYTECHNIC INSTITUTE
Department of Geology

Technical Report No. 5

63-2-4

Stress Propagation in Non-Linear Viscoelastic Materials: Numerical Calculations

Edward J. Mercado*

January 31, 1963

Prepared for:

Ballistic Research Laboratories

Aberdeen Proving Ground, Maryland

Technical Monitors

B. Perkins
A. A. Thompson

Contract No. DA-30-115-509-ORD-1009

Approved:

Samuel Katz

Samuel Katz
Project Supervisor

*Now at Gulf Research and Development Co., Pittsburgh, Pa.

ABSTRACT

The results of four digital computer calculations based on solutions by the method of characteristics of the equations for stress propagation in a nonlinear viscoelastic material, with a plane impulsive source, as given in two previous reports, are presented in graphical form. Many of the observed features of the variation of stress, strain, and particle velocity are reproduced by the theory, including an increase in elastic constants, as compared with static measurements, and the development of a plateau of constant residual strain near the impact face.

LIST OF SYMBOLS

σ - stress

V - particle velocity

ε - infinitesimal strain or space gradient of displacement

E - Young's modulus

a, b - dynamic constants of material

ρ - density

C - velocity of initial wave front

t - time

x - Lagrangian space variable

$g(\sigma)$ - function of stress

$g^{-1}(\varepsilon)$ - inverse function of stress

R, S - static constants of material

ACKNOWLEDGMENT

The author wishes to express his appreciation to Messrs. R. C. Makino and M. J. Romanelli of Ballistic Research Laboratories for programming the theory presented in Reference 1.

INTRODUCTION

The two previous reports[1,2] in this series are based on Malvern's theory[3,4] for stress propagation in strain-rate sensitive materials. They are concerned with the loading and unloading parts of a complete stress cycle and will be referred to as References 1 and 2. Reference 1 deals with the loading process and extends Malvern's theory to include finite-amplitude strains and an additional dynamic constant. These modifications provide a theoretical basis for predicting the residual strain distributions and the increase in Young's modulus that are observed experimentally from the dynamic testing of soils and of some metals. Reference 2 is primarily concerned with the unloading process and qualitatively traces the change in shape of a rectangular stress pulse applied at $x = 0$ as it propagates into the material, under the assumption of a linear unloading law. The theory is extended to include nonlinear unloading laws. Numerical procedures are given for calculating the variation of stress, strain, and particle velocity during the complete stress cycle.

This report presents graphically and analyzes the results of the computations performed at Ballistic Research Laboratories to date. One set of calculations is based on static stress-strain data for the Fort Peck Sand as determined by Whitman,

et al[5]. Two sets of empirically determined dynamic constants are utilized in these calculations, one based on a value suggested by Parkin[6]; the other is empirically determined to compare qualitatively with dynamic tests on copper reported by Kolsky and Douch[7]. The calculation is repeated with the second set of dynamic constants, utilizing a different form for the static stress-strain law.

Another computation, based on physical parameters representative of dune sand, is compared to numerical results from an approximate analytical solution derived in Ref. 1. This comparison shows that over a considerable range of time and distance, the approximate analytical solution yields results within several per cent of the solution calculated by the digital computer.

Based on the calculations for the Fort Peck Sand, the residual strain distribution under the assumption of a linear unloading law of the form $\varepsilon - \sigma/\rho c^2$ is evaluated for various pulse widths. There is qualitative agreement between these calculations and residual strain distributions observed in copper when the rise time-to-pulse width ratio is approximately the same between theory and experiment.

FORT PECK SAND

Physical Constants

The static stress-strain response of the Fort Peck Sand, experimentally determined by Whitman, et al[5], is shown in Figure 1. Young's modulus measured as the initial slope of this curve is (14.7) 10^8 dynes/cm^2, and the density is reported as 1.60 gm/cm^3. An analytical representation of the static stress-strain curve is obtained by fitting an empirical formula suggested by Osgood[8] of the form (Ref. 1, eq. 2)

$$\varepsilon = \frac{\sigma}{E} + R\left(\frac{\sigma}{E}\right)^S \qquad (1)$$

to the static data. The constants R and S in (1) may be determined by plotting log ($\varepsilon - \sigma/E$) vs. log (σ/E) and fitting a straight line through the resulting points. The slope and intercept of this straight line are S and log R, respectively. The constants R and S evaluated in this manner are (6.86) 10^3 and 2.22. With these values, (1) adequately fits the data over the range of interest and is shown superimposed on the experimentally determined stress-strain curve in Figure 1.

With (1) as the static stress-strain law, the basic constitutive equation defining the material (Ref. 1, Eq. 10)

takes the form

$$\sigma_t - \frac{b}{a}\varepsilon_t = \frac{1}{a}\left[\varepsilon - g(\sigma)\right] \qquad (2)$$

If this is interpreted as an elastic-plastic law as in Malvern's work, the elastic strain rate is $\varepsilon'_t = \frac{a}{b}\sigma_t$, while the simultaneously occurring plastic strain rate is

$$\varepsilon''_t = \varepsilon_t - \varepsilon'_t = \frac{1}{b}\left[g(\sigma) - \varepsilon\right] .$$

Thus, the plastic strain rate is assumed proportional to the difference between the instantaneous strain and the strain which would result if the instantaneous stress had been statically applied. In Malvern's theory, the plastic strain rate was a function of the difference between the instantaneous stress and the stress the material would support if the instantaneous strain had been produced statically.

To gain some insight into the difference between these alternative expressions for the plastic strain rate, calculations were performed using identical boundary conditions and physical constants--first using (1) as the static law and, second, solving (1) for σ so that (2) was proportional to

$$\left[\sigma - \bar{g}'(\varepsilon)\right] .$$

There are no experimental data known to the author from which the dynamic constants a and b may be directly determined. However, it is known from theory that $b/a \geq E$. On the basis

of this relation, b/a is arbitrarily chosen as (14.9) 10^8 dyne/cm^2, which yields an initial wave front velocity of 12,000 in/sec. One set of dynamic constants is found by assuming $1/a = (6.5)10^3$, as suggested by Parkin[6] from an empirical study of Whitman's data. This yields b = 3.32308. The calculation using these constants and (1) as the static law is referred to as Case I. This value of b applies to a hypothetical material that approaches its equilibrium state very slowly, as is illustrated by the fact that at x = 0, almost 7 seconds are required for the material to reach 90% of the ultimate strain. Since such slow flow is not observed experimentally in soils and metals, another value for b may be obtained by requiring the strain to reach 90% of its ultimate value in 0.005 second. By setting $\varepsilon(0, 0.005) = .9\, g(\sigma_0)$ and solving for b (Ref. 1, Eq. 42), one obtains

$$b = -0.005 \Big/ \log\left\{0.1/\left(1 - \varepsilon_0/g(\sigma_0)\right)\right\} \qquad (3)$$

$$= (2.38969)10^{-3}$$

By requiring the initial wave-front velocity to be 12,000 in/sec, one obtains $a = b/\rho C^2 = (1.10633)10^{-7}$. The calculation using these more realistic values for a and b with (1) as the static law is referred to as Case II. The calculation with the

dynamic constants for Case II and the static law written as $[\sigma - g^{-1}(\varepsilon)]$ is referred to as Case III.

Step Response

The response of the Fort Peck Sand to a step in stress of 50 lbs/in^2 applied at x = 0 is numerically evaluated for the above two sets of dynamic constants and two different forms for the static law. These solutions are compared to the centered simple wave solution obtained by neglecting time-rate effects. The present formulation does not distinguish between an initial tensile or compressive stress. A tensile stress is assumed positive along the outward normal corresponding to the negative x direction. The resulting particle velocity is parallel to the stress, but is negative in sign since the velocity vector is determined relative to the coordinate system. A positive velocity would correspond to a compressive stress.

Contours of constant stress, strain, and particle velocity using the set of dynamic constants of Case I (Figs. 2, 3, and 4) show the initial, slowly-decaying, discontinuous elastic wave-front, followed by a region in which the stress, strain, and particle velocity increase toward their respective limits. In this region, lines of constant amplitude are not straight; however, their deviation from linearity is small

over a considerable range of amplitude and strain rate. Because of this, the resulting contour patterns resemble a simple wave originating from some unknown origin.

The calculation is repeated using the second set of dynamic constants (Case II). These constants essentially contract the time scale compared to Case I, resulting in a much closer approximation to the centered simple wave solution, and in better agreement with strain records obtained from a soil shock tube. The resulting contours of stress, strain, and particle velocity (Figs. 5, 6, and 7) show that the initial, discontinuous wave-front decays quite rapidly, subsiding to half its initial amplitude after approximately 14 inches. As in Case I, lines of constant amplitude behind the initial wave front are not quite straight. These limited calculations suggest that, except for the infinite strain rates associated with discontinuities, phase velocities are relatively more sensitive to strain amplitude than to strain rate.

As indicated above, the Case III calculation (Figs. 8, 9, 10) differs from the Case II calculation only in assuming the plastic strain rate proportional to the stress difference rather than the strain difference. Comparison of the contour patterns for these two cases shows that the material approaches equilibrium much more rapidly when the plastic strain rate is taken pro-

portional to the strain difference . This may be explained by interpreting the characteristic equations for a nonlinear viscoelastic material (Ref. 1, Eqs. 23, 24, and 25) as a perturbation of the corresponding plastic equations and noting that the perturbing term ($g(\sigma) - f(\varepsilon)$) is in general numerically smaller when written as a strain difference [i.e., $(g(\sigma) - \varepsilon)$] than when written as a stress difference [i.e., $(\sigma - f(\varepsilon))$]. As the perturbing term approaches zero, the solution should approach the simple wave solution.

For purposes of comparison, the centered simple wave solution based on the static stress-strain law (1) is shown in Figure 11. Since it is based on the rate-independent plastic wave theory, it may be directly compared to the calculations for all three cases.

Residual Strain Distributions

A commonly accepted procedure[3,9] for calculating the residual strain distribution is to assume linear unloading parallel to the initial slope of the loading cycle. Under this assumption, the residual strain distribution resulting from a rectangular stress pulse, t_o seconds in duration, is (Ref. 2, eq. 13)

$$\varepsilon_{res} = \varepsilon(t_o, t_o + X/c) - \frac{\alpha}{b}\sigma(t_o, t_o + X/c) \quad (4)$$

With the loading cycle calculated from the rate-independent theory, the residual strain produced by a rectangular stress pulse of variable duration shows the familiar plateau of constant strain[7] near the impact boundary x = 0 (Fig. 12). Beyond this plateau, the residual strain rapidly approaches zero.

Residual strain distributions for Case I, determined by applying (4) to the Fort Peck Sand, are shown in Figures 13 to 15 for a rectangular stress pulse of duration 1, 4, and 10 seconds respectively. These results differ markedly from those based on the rate-independent theory since no plateau of constant residual strain is developed.

The residual strain distributions based on the Fort Peck Sand (Case II) are shown in Figures 16 to 19 for pulses of 10, 20, 30 and 40 milliseconds, respectively. A plateau of almost constant strain develops close to x = 0 for a pulse duration which is several times greater than the rise time. For this calculation, the rise time is arbitrarily chosen as the time required to attain 90% of the ultimate strain — 0.005 second. Thus the observed plateau of constant residual strain is predicted in viscoelastic theory, if appropriate values of the dynamic constants are chosen and if the pulse is long

enough for the material near the impact face to approach equilibrium.

Residual strain distributions resulting from impact tests on copper bars have been reported by Kolsky and Douch[7] (Fig. 20). The dynamic constants for the Case II calculation were determined empirically in an attempt to reproduce these residual strain distributions. This was done by observing that the ratio of rise time to pulse duration for the experimentally recorded pulses (Fig. 21) which produced these residual strain distributions was of the order of four to five. The residual strain distributions calculated from Case II, where the corresponding ratio is of this order of magnitude, are qualitatively similar in form (Figs. 18 and 19).

Physical Constants

Typical values for dune sands as reported by Heiland[10] are ρ = 1.76 gm/cm^3, 1.64 $\leq 10^{-8}E \leq$ 3.69 dynes/cm^2. The ratio b/a is chosen as (3.69) 10^8 dynes/cm^2 and E as (1.64) 10^8 dynes/cm^2. The constant $\underline{b}$ is calculated by assuming Malvern's value 1/a = 10^6 for metals, yielding $\underline{b}$ = 7.7. This calculation was performed to evaluate the validity and usefulness of an approximate solution (Ref. 1, pp. 23-28), which utilizes a static stress-strain curve of the form (1) with S = 2.0 for mathematical simplicity. Another restriction on the approximate solution requires that the constant R be determined from the relation

$$\frac{a}{\sigma} = \frac{1}{E} + \frac{2R\sigma_0}{E^2} \qquad (5)$$

With σ_0 = 50 lbs/ft^2 as one boundary condition and the previously determined constants, R =(5.54)10^{-3}.

Step Response

Contours of constant stress, strain, and particle velocity from digital computer data again show a simple wave pattern from an unknown origin (Figs. 22, 23, and 24).

The solutions calculated by the digital computer are replotted to facilitate comparison with data from the approxi-

mate solution. Figures 25-28 show values for stress and strain as functions of the digitized "reduced time" n, calculated from these two methods at representative intervals. The arrival of the initial discontinuous wave front is represented by n = 0, and each integer thereafter represents a time interval of 0.05 second. Thus n = 15 corresponds to a pulse width of 0.75 second.

One of the basic assumptions inherent in this approximate solution restricts its region of validity to small "reduced times"; i.e., small n. As can be seen from Figures 25 - 28, the two solutions are identical at n = 0 and diverge slowly with increasing n. The percentage errors for stress and strain over the range of available data have been calculated and the contours of constant percentage plotted (Figs. 29 and 30). These figures show that the maximum error for stress over the range of data examined is slightly over 0.3%. The maximum error for strain over this same range of data is slightly over 7%. This calculation is deliberately extended beyond its expected range of application since n = 15 corresponds to a loading pulse considerably longer in duration than an actual explosion or dynamic test. These approximate solutions should be valid within a few per cent over the range of pulse durations normally encountered. The use of other values of a and b should not greatly alter the general conclusions outlined above.

COMPARISON WITH PLASTIC WAVES IN METALS

Stress-Strain Curves

Kolsky and Douch have determined the dynamic and static stress-strain curves for an aluminum alloy, pure aluminum, and copper (Figs. 31, 32 and 33). The tests on an aluminum alloy (Fig. 31) show that the values of stress and strain determined dynamically scatter evenly about the static curve. This alloy belongs to the class of strain-rate insensitive materials which are well-described by the Von Karman-Taylor[9] plastic wave theory.

Similar dynamic tests on pure aluminum show that it is strain-rate sensitive (Fig. 32). However, there is no discernible difference between the dynamic and static Young's modulus. This may be interpreted in terms of the nonlinear viscoelastic theory (Ref. 1) as requiring only one dynamic viscoelastic constant. Thus it should be possible to describe the dynamic behavior of pure aluminum by Malvern's theory, utilizing only one dynamic constant.

On the other hand, the dynamic and static stress-strain curves for pure copper show a small but significant increase in Young's modulus under dynamic test conditions (Fig. 33). This increase in Young's modulus suggests that at least two dynamic constants are required to describe adequately the dynamic behavior of copper, as outlined in Reference 1.

The data from which these dynamic stress-strain curves are constructed would be obtained from gages located at various distances from the impact face. Since, for strain-rate sensitive materials, there is no one-to-one correspondence between stress and strain, the stress-strain curve deduced from experimental data will be a function of recording position. To gain some insight into the importance of recording position, the stress-strain curves obtained from the calculations of Cases I and II for the Fort Peck Sand are shown in Figures 34 and 35 for various distances from the impact face. There is an apparent increase in the yield point, which decreases with distance from the origin, and in Young's modulus. Above the apparent yield point, the dynamic curve roughly parallels the static curve giving the appearance of shifting the entire static curve upward. The calculation for Case II shows that for distances greater than 12 inches, the apparent stress-strain curve varies slowly with small changes in recording position.

SUMMARY

The theory presented previously (Ref. 1) for stress propagation in nonlinear viscoelastic materials, assuming infinitesimal strain, has been programmed for a digital computer. The resulting calculations have been used to predict the mechanical parameters of stress, strain, and particle velocity as a function of time and distance from an impulsive plane wave source. By suitable choice of the dynamic constants, the solution can be made to approximate a simple wave. Such observed features as an increase in Young's modulus and a plateau of constant residual strain at the impact boundary are reproduced by the theory.

Three calculations were performed, permitting comparison of the effect on wave shape of different dynamic constants. The first two calculations (Cases I and II) assumed that the plastic strain-rate is proportional to the difference between the instantaneous strain and the strain which would result if the instantaneous stress had been statically applied. The dynamic constants of Case I were altered for the calculations of Case II, to give predictions in closer agreement with experimental data. In the third calculation (Case III) the plastic strain rate was taken proportional to the difference between the instantaneous stress and the stress required

to produce the instantaneous strain statically. These calculations indicate that the former assumption results in a more rapid approach to values that would be obtained under static conditions.

The results of an approximate analytical solution (Ref. 1) are compared to the numerical solution from the digital computer. Although dynamic constants chosen for this calculation were not physically meaningful, the results indicate that the approximate solution, within its limits of validity, yields results which are sufficiently exact over the range of time and distance of interest for most applications.

From the work of Kolsky and Douch, metals appear to fall into three classes, depending upon the number dynamic constants required to describe their behavior. Materials such as certain aluminum alloys are not strain-rate sensitive and thus no dynamic constants are required for describing their behavior under impact. Pure aluminum requires only one dynamic constant, since Young's modulus is the same under static and dynamic conditions. On the other hand, pure copper appears to require two dynamic constants to account for the increase in Young's modulus observed under dynamic conditions.

REFERENCES

1. Mercado, E. J., "Stress Propagation in Nonlinear Viscoelastic Materials", Tech. Rept. No. 3, Ballistic Research Laboratories, Contract No. DA-115-509-ORD-1009, May 1, 1962 (Ref. 1)

2. Mercado, E. J., "Stress Propagation in Nonlinear Viscoelastic Materials", Tech. Rept. No. 4, Ballistic Research Laboratories, Contract No. DA-115-ORD-1009, October 1962 (Ref. 2)

3. Malvern, L. E., "Plastic Wave Propagation in a Bar of Material Exhibiting a Strain-Rate Effect", Quart. of Appl. Math., Vol. 8, No. 4, January 1950.

4. Malvern, L. E., "The Propagation of Longitudinal Waves of Plastic Deformation in a Bar of Material Exhibiting a Strain-Rate Effect", Trans. ASME, Jour. Appl. Mech., Vol. 18, p. 203, 1951.

5. Whitman, R. V., et al., "The Behavior of Soils Under Dynamic Loading", Final Report on Laboratory Studies, MIT, Department of Civil and Sanitary Engineering, Soil Mechanics Laboratory, August 1954, AFSWP-118, Contract DA-49-129-Eng-227, Office of the Chief of Engineers.

6. Parkin, Blaine R., "Impact Waves in Sand: Theory Compared with Experiment on Sand Columns", Proc. of the Am. Soc. of Civil Engrs., Jour. of the Soil Mechs. and Found. Div., Vol. 87, No. SM3, June 1961.

7. Kolsky, H., and Douch, L. S., "Experimental Studies in Plastic Wave Propagation", Jour. Mech. Phys. Solids, 10, 195-223, 1962.

8. Osgood, W. R., "Stress-Strain Formulas", Jour. of the Aero. Sciences, pp 45-48, January 1946.

9. Lee, E. H., "A Boundary Value Problem in the Theory of Plastic Wave Propagation", Quart. Appl. Math. 10, p 335, 1953.

10. Heiland, C. A., "Geophysical Exploration", Prentice Hall, Inc., p 469, 1946.

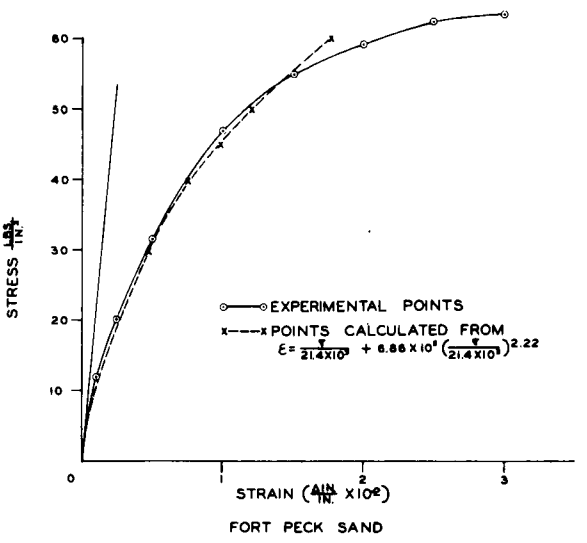

Figure 1

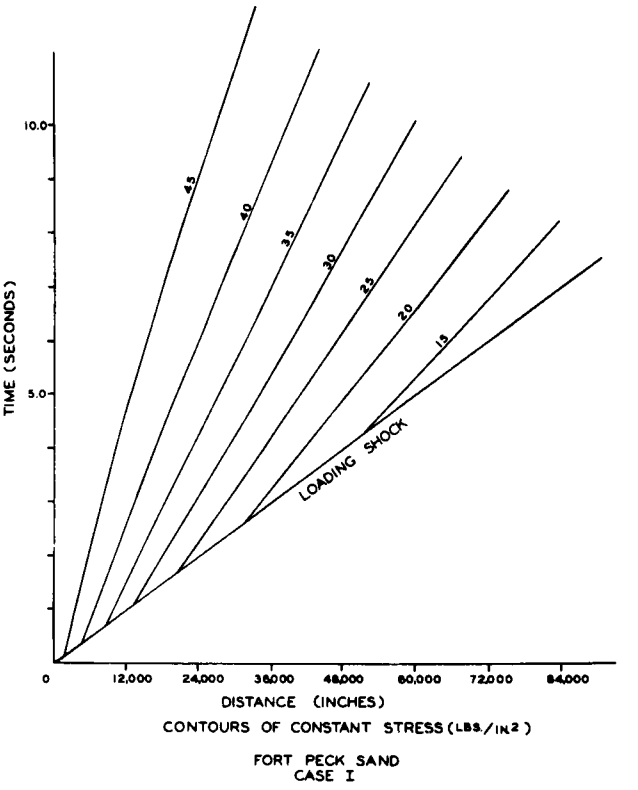

Figure 2

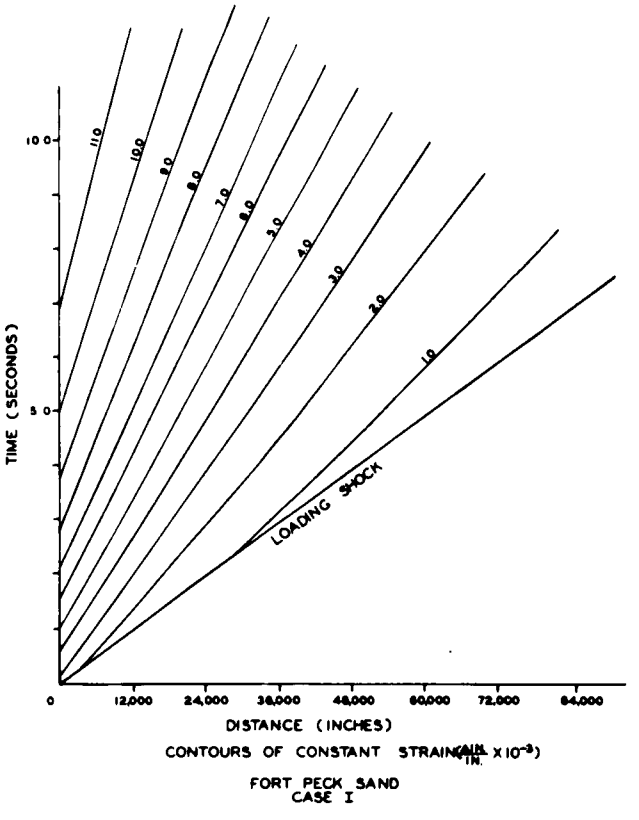

Figure 3

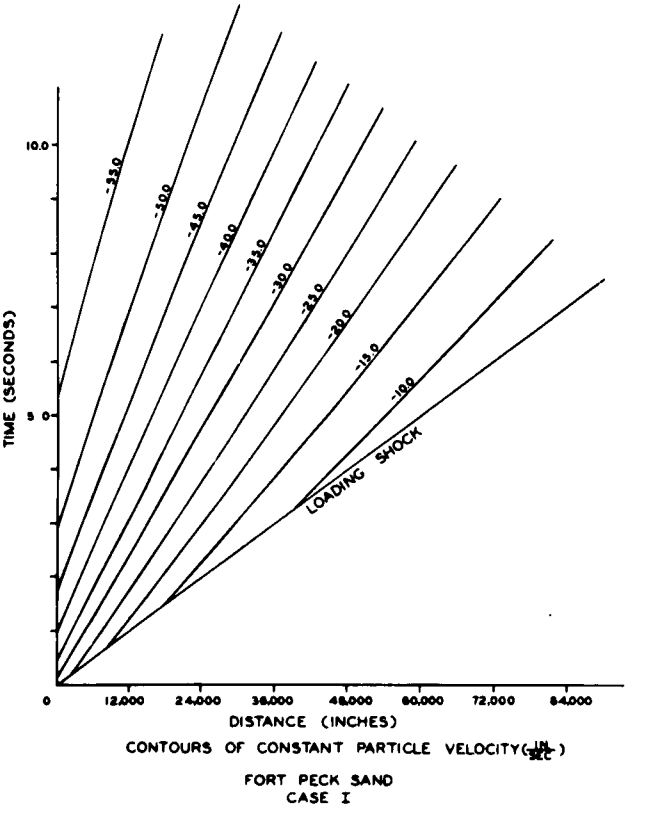

Figure 4

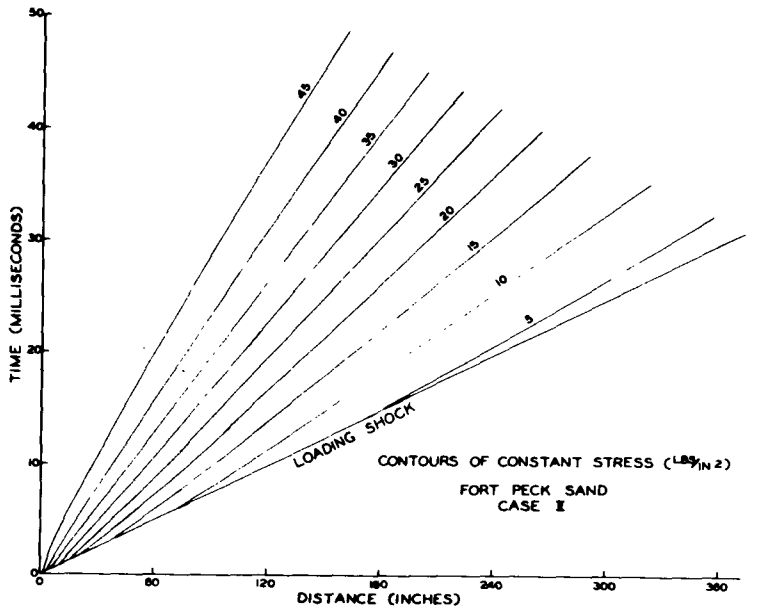

Figure 5

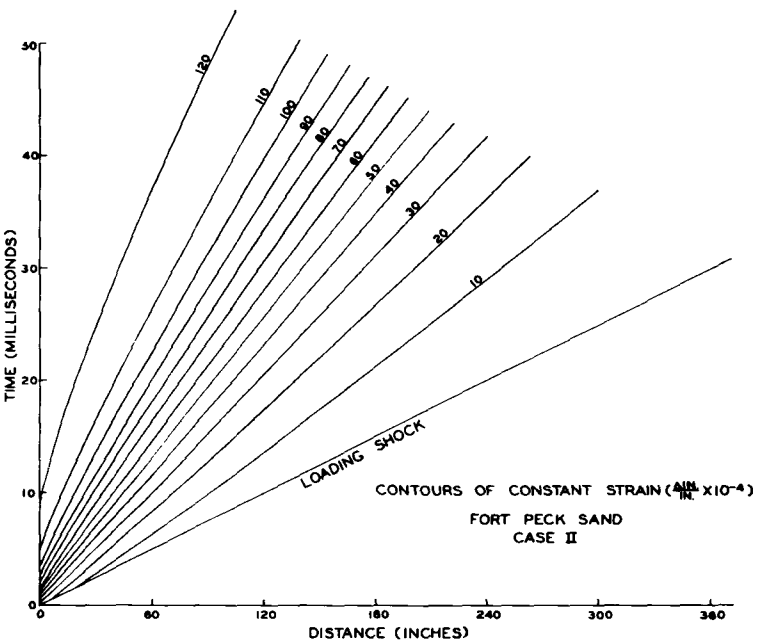

Figure 6

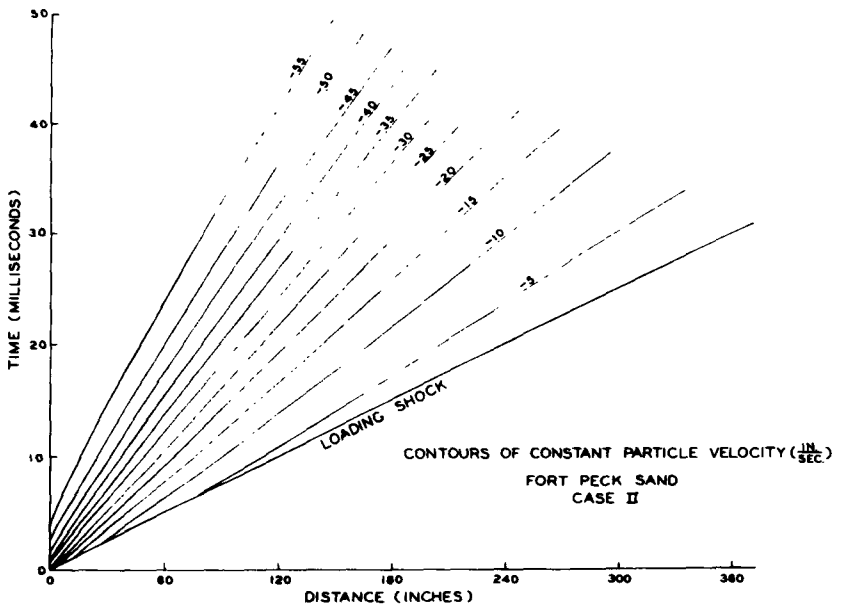

Figure 7

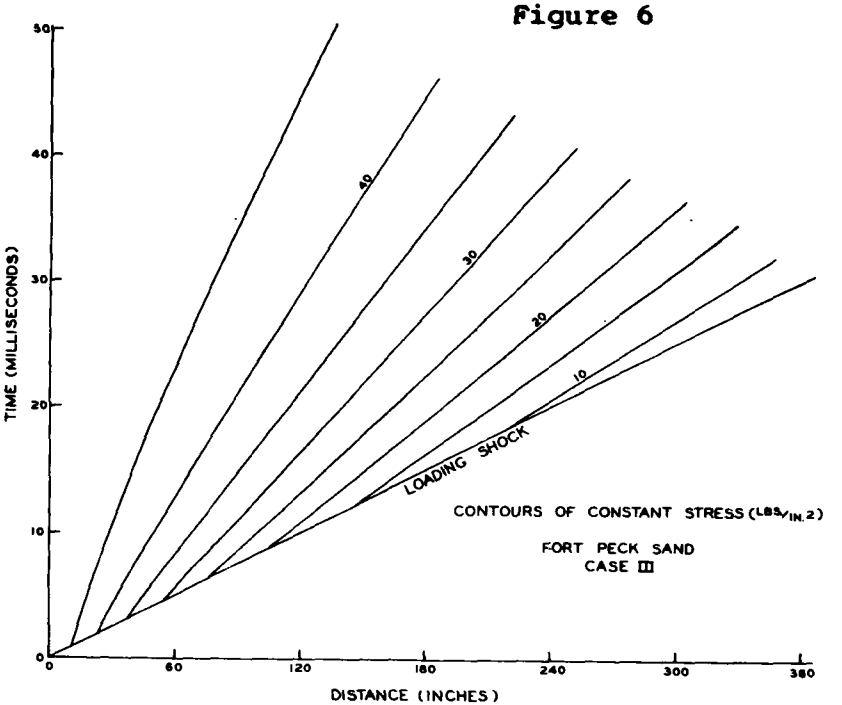

Figure 8

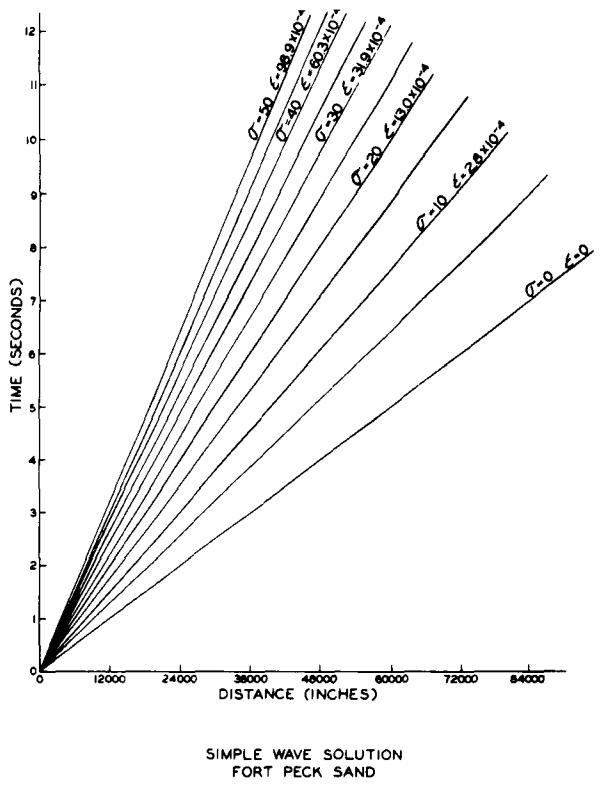

Figure 9

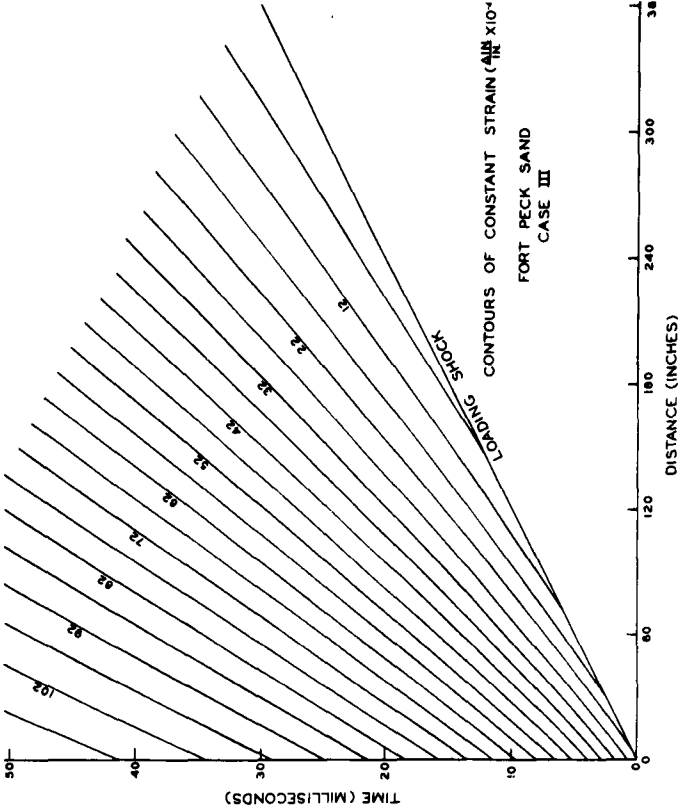

Figure 10

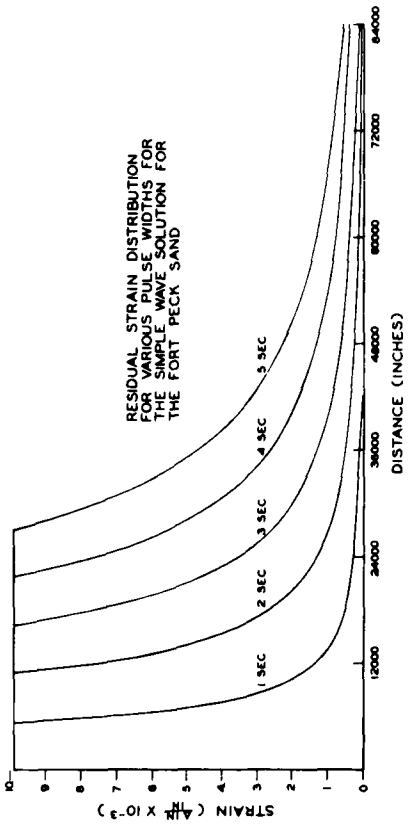

Figure 11

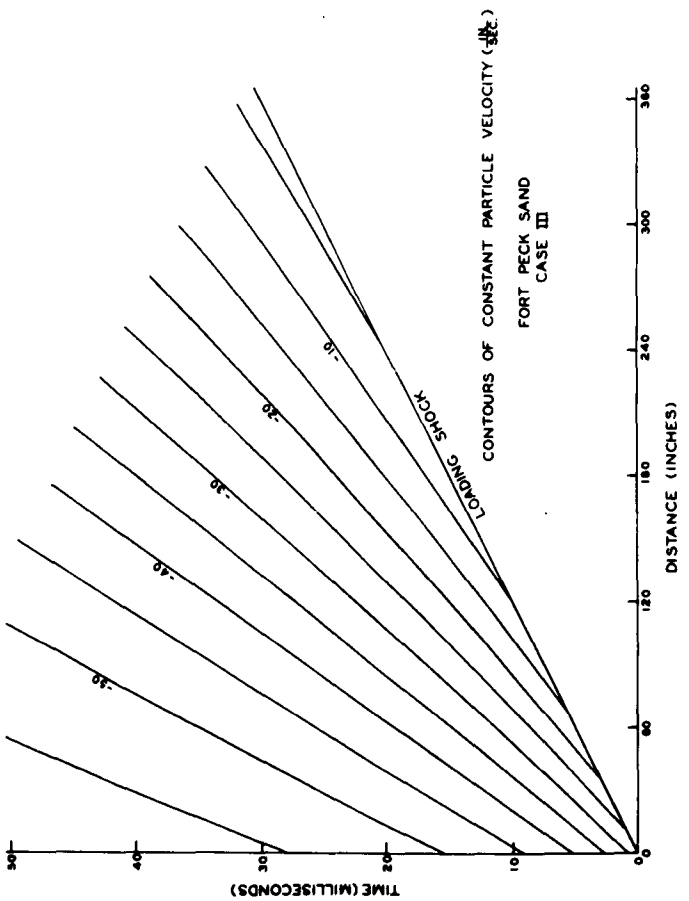

Figure 12

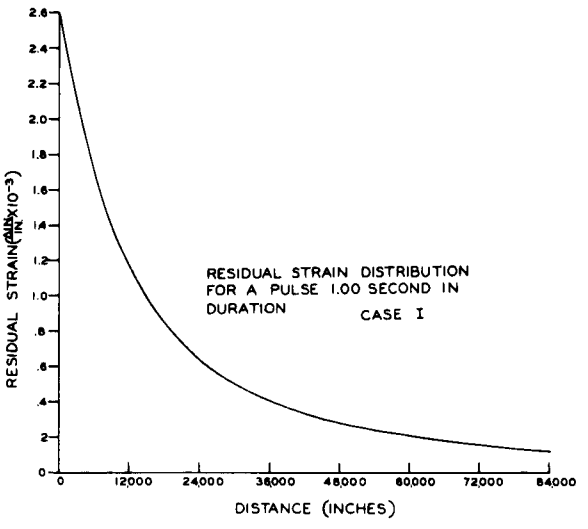

Figure 13

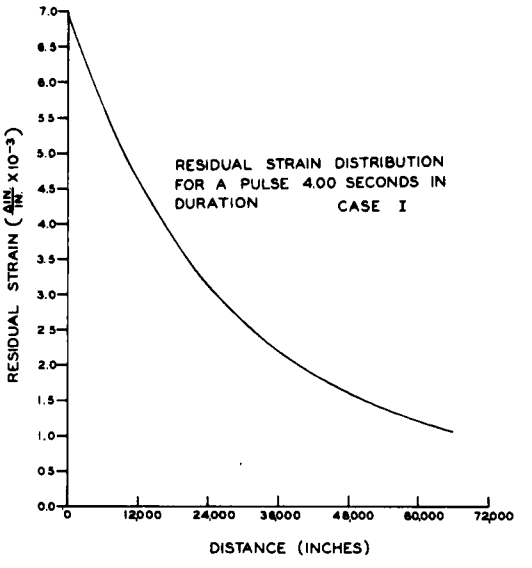

Figure 14

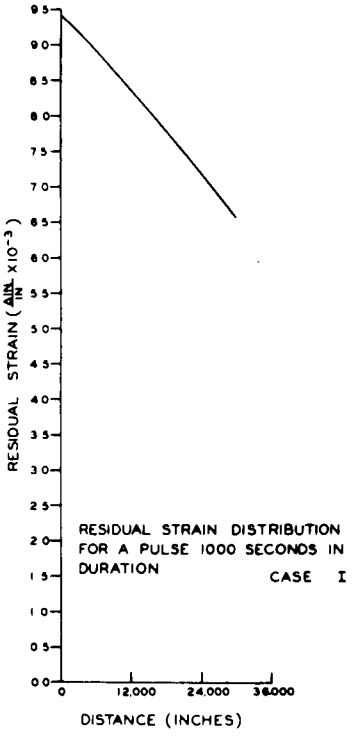

Figure 15

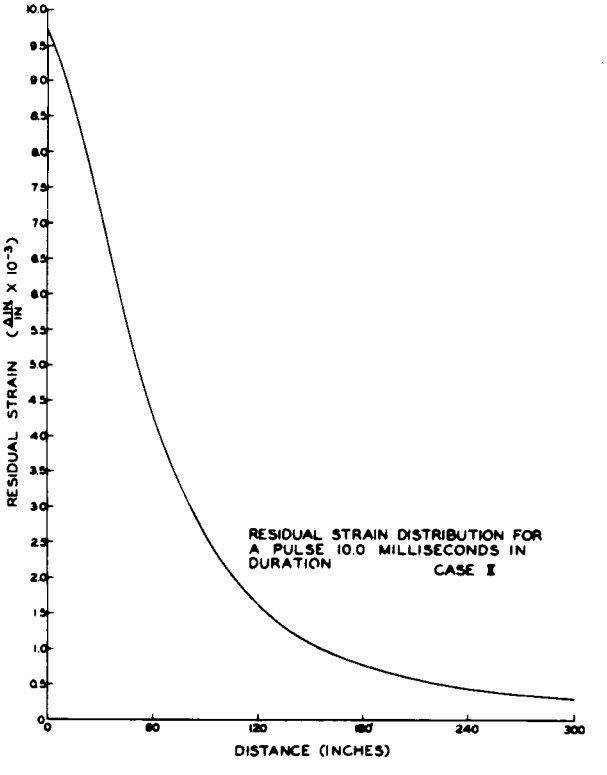

Figure 16

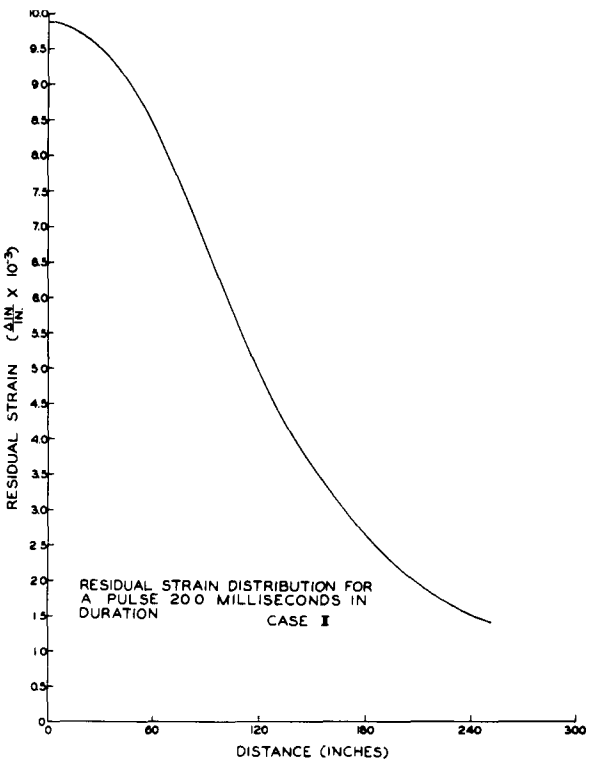

Figure 17

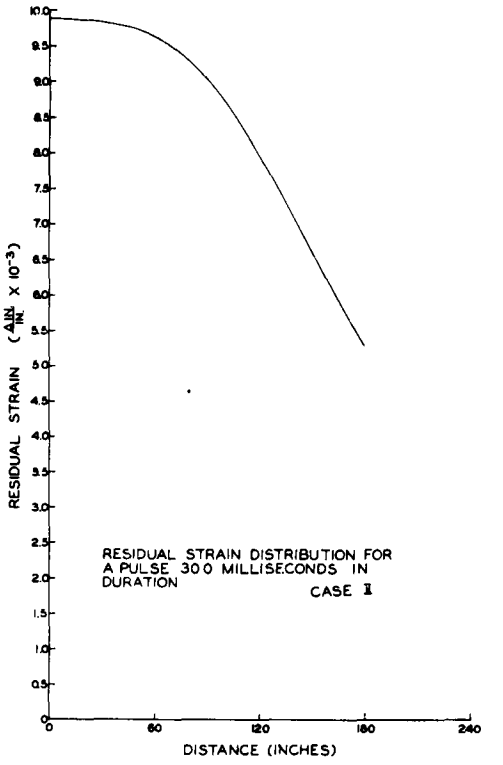

Figure 18

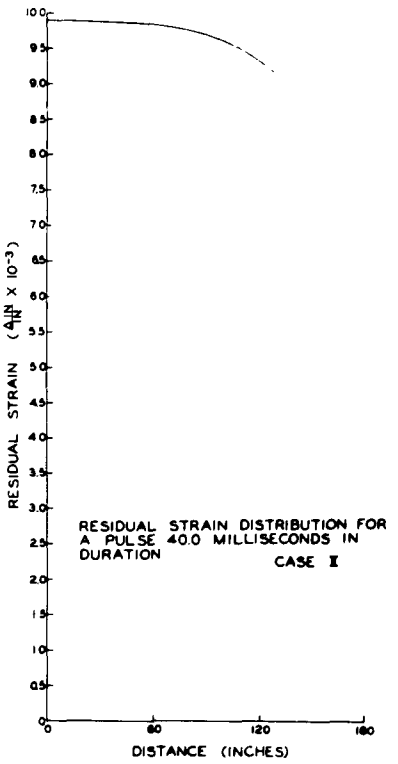

Figure 19

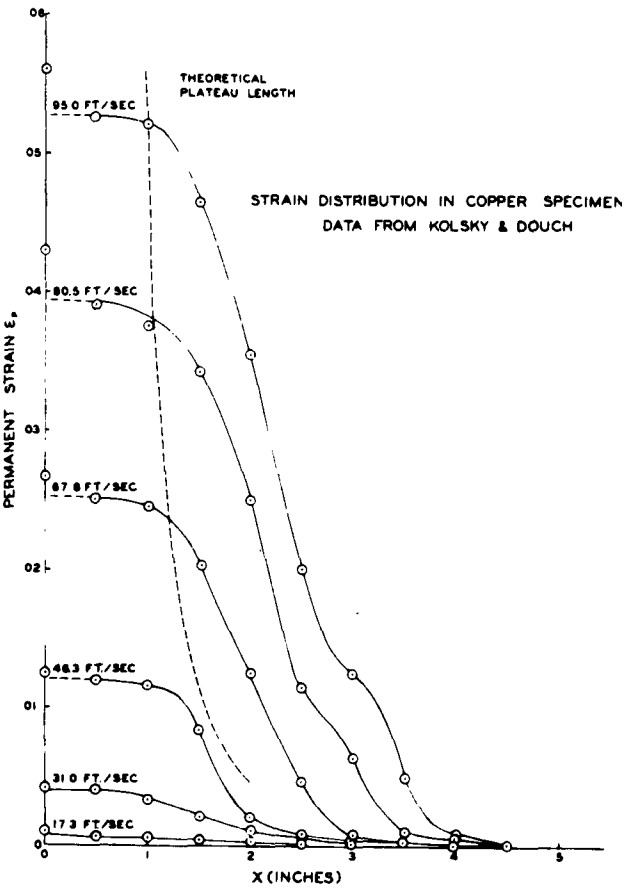

Figure 20

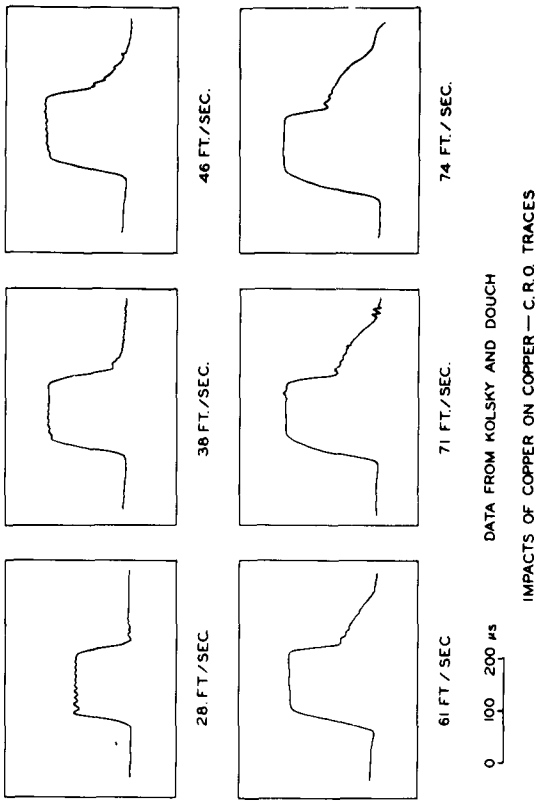

Figure 21

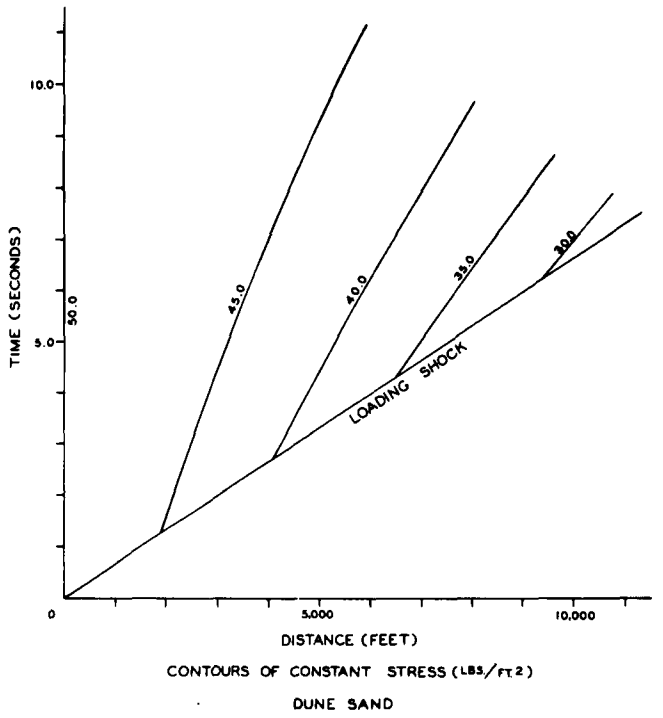

Figure 22

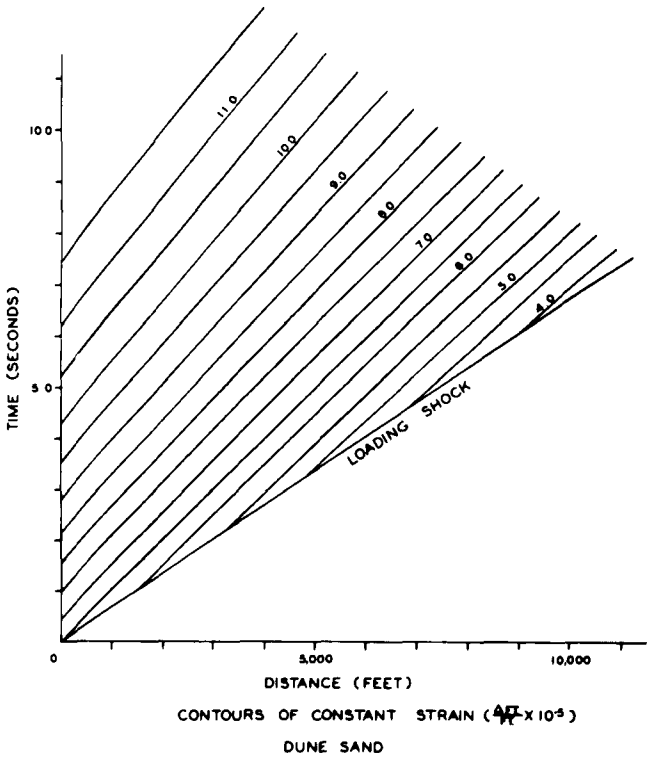

Figure 23

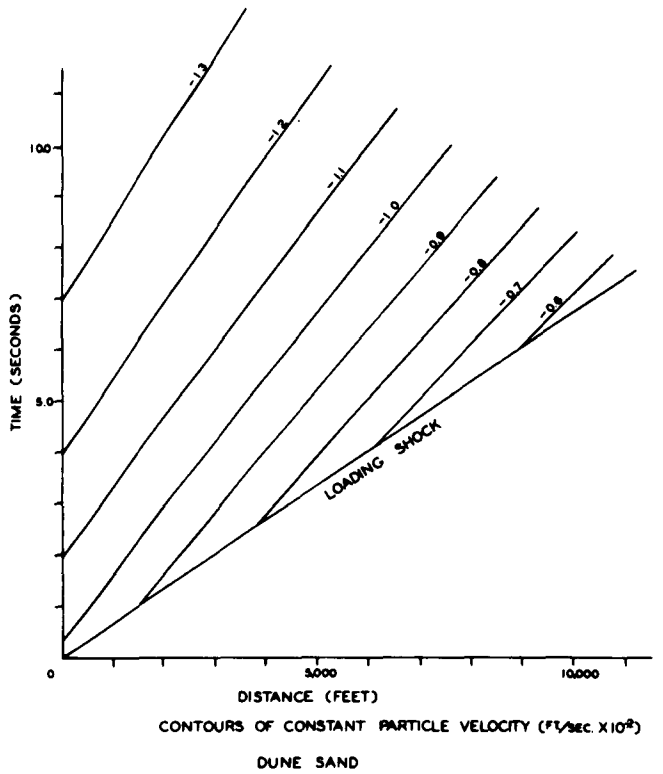

Figure 24

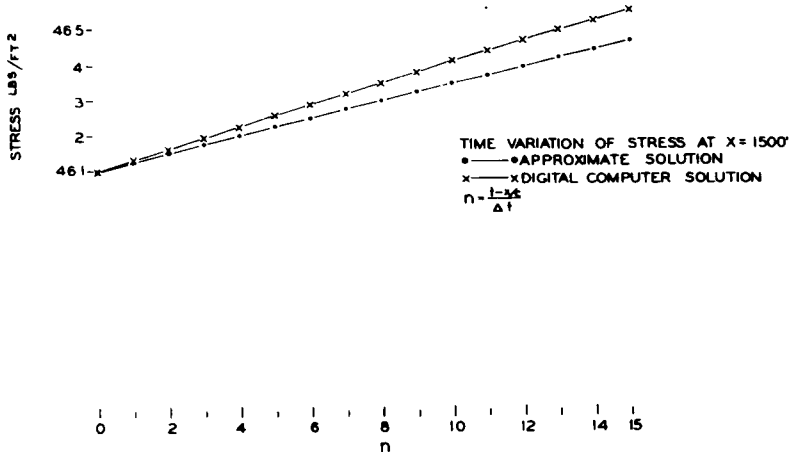

Figure 25

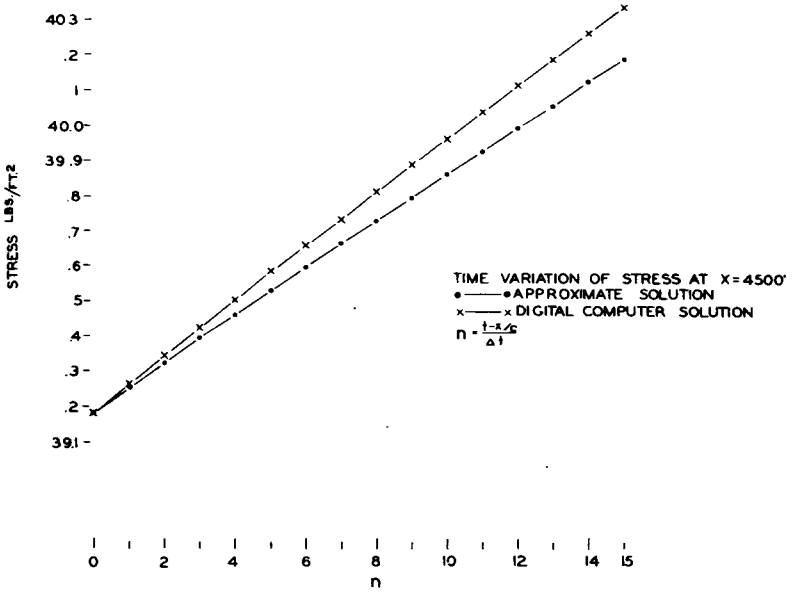

Figure 26

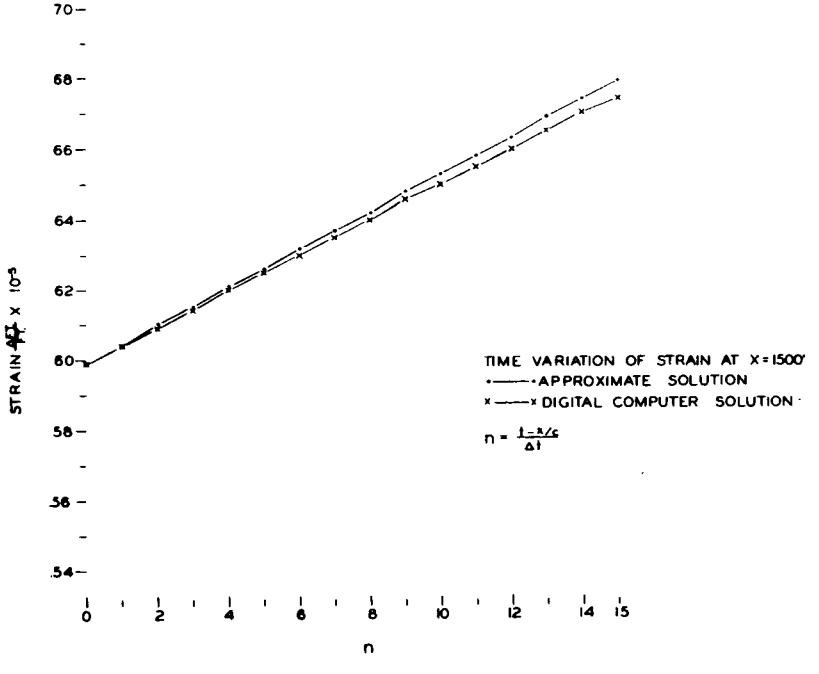

Figure 27

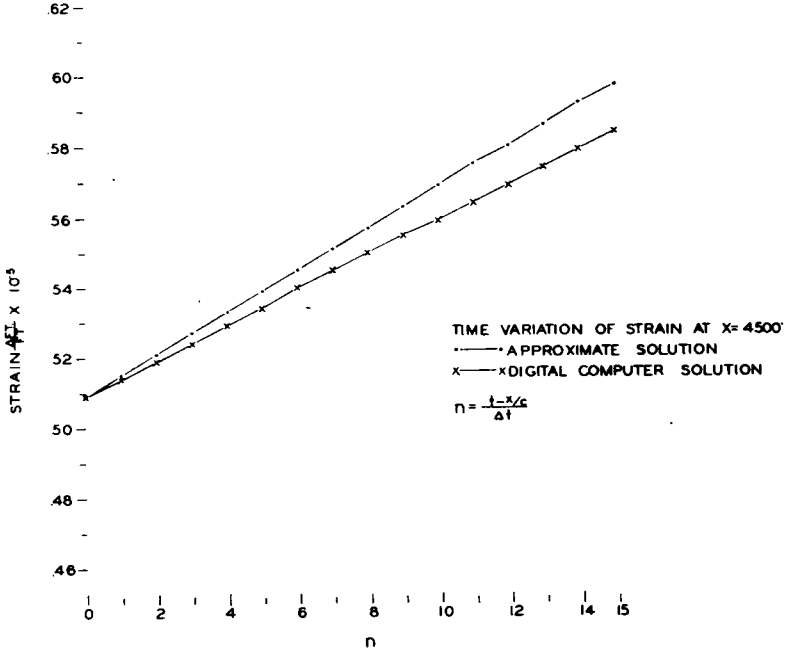

Figure 28

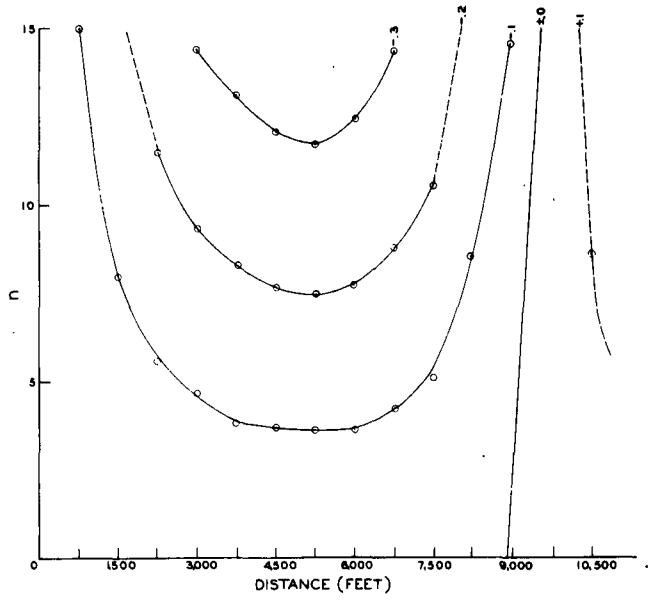

ERROR IN STRESS
CONTOUR INTERVAL 0.1%

Figure 29

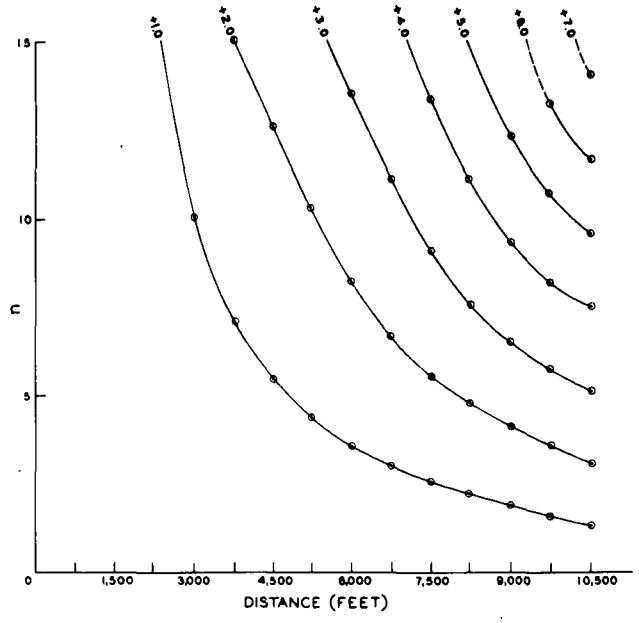

ERROR IN STRAIN
CONTOUR INTERVAL 1.0%

Figure 30

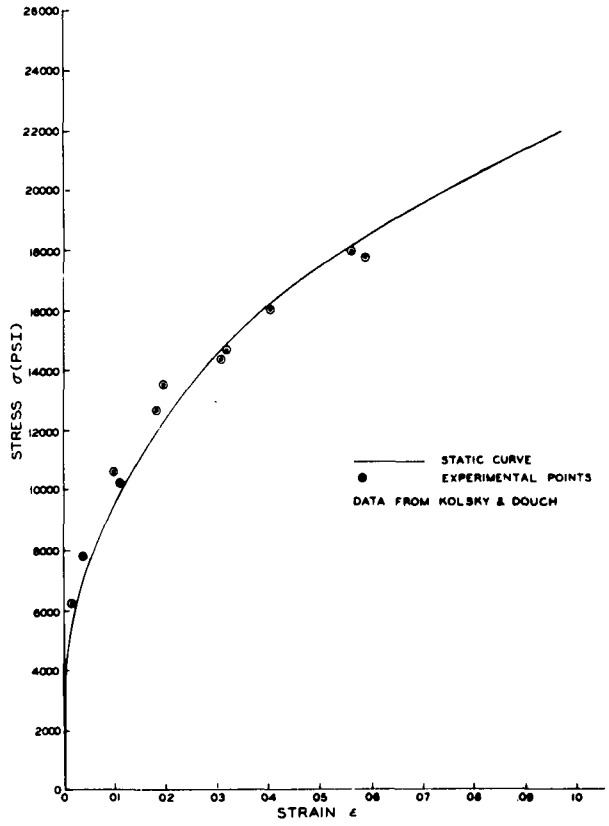

STRESS-STRAIN CURVE FOR ALUMINUM ALLOY

Figure 31

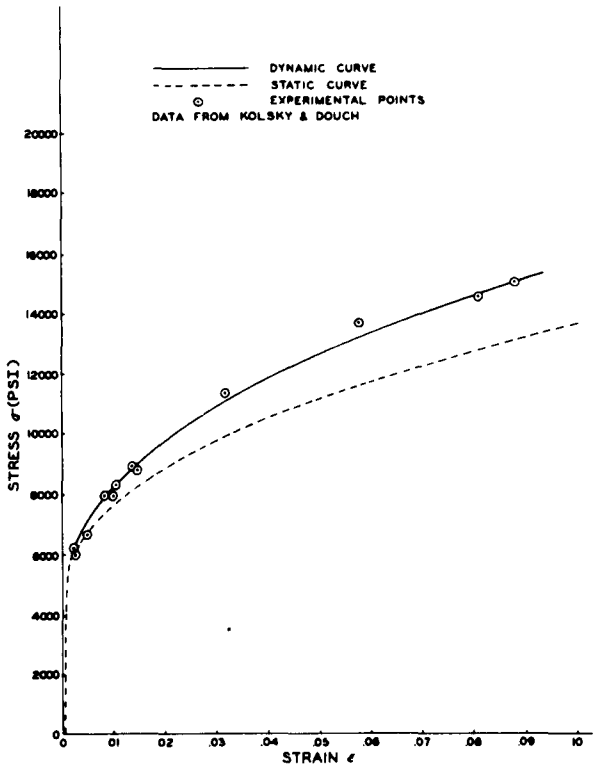

STRESS-STRAIN CURVES FOR ALUMINUM

Figure 32

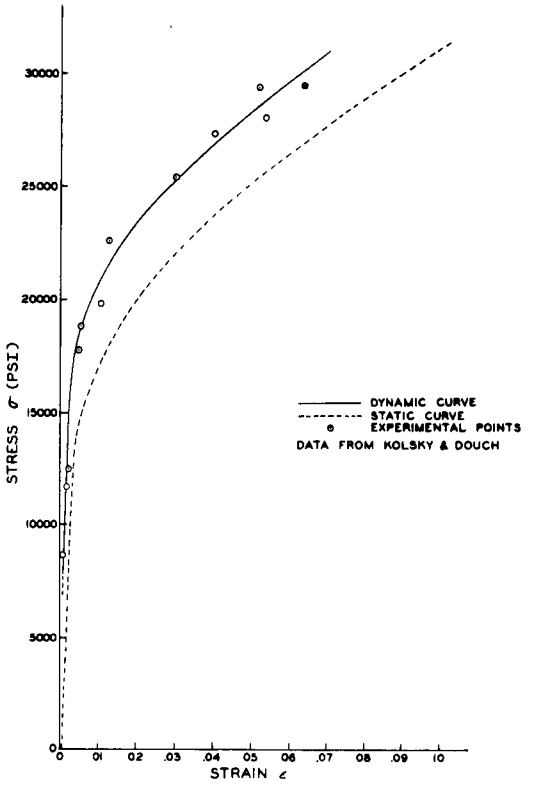

STRESS-STRAIN CURVES FOR COPPER

Figure 33

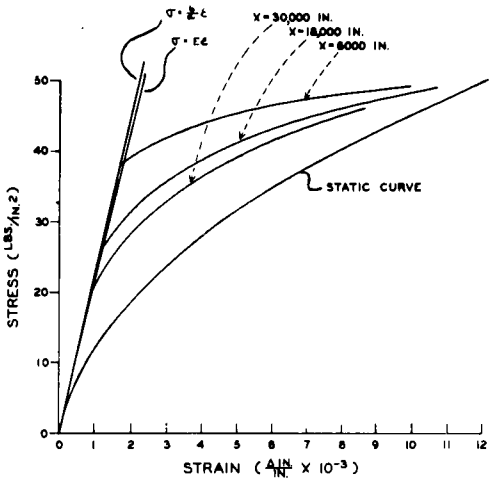

APPARENT STRESS-STRAIN CURVES
FOR VARIOUS DISTANCES FROM THE ORIGIN

FORT PECK SAND, CASE I

Figure 34

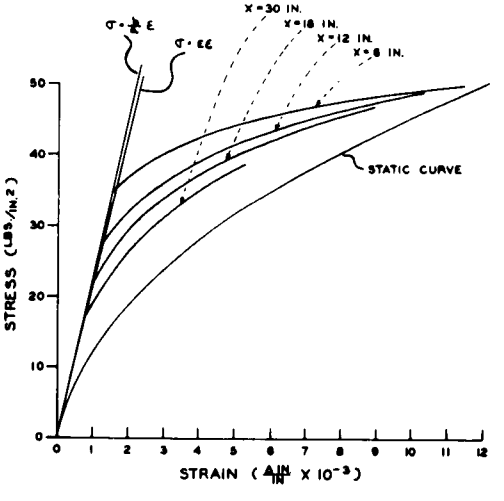

APPARENT STRESS-STRAIN CURVES
FOR VARIOUS DISTANCES FROM THE ORIGIN

FORT PECK SAND, CASE II

Figure 35

DISTRIBUTION LIST

for

TECHNICAL AND FINAL REPORTS

Rensselaer Polytechnic Institute
Contract No. DA-30-115-509-ORD-1009

No. of Copies	Organization
1	Chief of Ordnance Department of the Army Washington 25, D. C. Attn: ORDTB - Bal Sec
1	Commanding Officer Diamond Ordnance Fuze Laboratory Washington 25, D. C. Attn: ORDTL-012
10	Director Armed Services Technical Information Agency Arlington Hall Station Arlington 12, Virginia Attn: TIPCR
6	British Joint Services Mission 1800 K. Street, N. W. Washington 25, D. C. Attn: Reports Officer
3	Canadian Army Staff 2450 Massachusetts Avenue Washington 8, D. C.
2	Chief, Bureau of Naval Weapons Navy Department Washington 25, D. C. Attn: RRE
2	Chief of Naval Research Department of the Navy Washington 25, D. C. Attn: Code 118
1	Commanding Officer Naval Proving Ground Dahlgren, Virginia
2	Commander Naval Ordnance Laboratory White Oak Silver Spring, Maryland Attn. Mr. J. F. Moulton, Jr.
2	Director Naval Research Laboratory Anacostia Station Washington 20, D. C.
1	Officer in Charge Naval Civil Engineering Research & Evaluation Lab. Naval Station Port Hueneme, California Attn: Mr. J. Algood
1	Chief, Bureau of Yard and Docks Department of the Navy Washington 25, D. C. Attn: Cmdr. Saunders
1	Chief of Naval Operations Department of the Navy Washington 25, D. C. Attn: Op-36
1	Commanding Officer & Director David W. Taylor Model Basin Washington 7, D. C. Attn: Structural Mechanics Div.

Distribution List (Cont'd)

No. of Copies	Organization
1	Director Air University Library U. S. Air Force Maxwell Air Force Base Alabama
2	Commander Naval Ordnance Test Station China Lake, California Attn: Technical Library Editorial Section
1	Deputy Chief of Staff - Development Research & Development Directorate U. S. Air Force Washington 25, D. C. Attn: Major E. Lowery
2	Commanding General Special Weapons Command Kirtland Air Force Base Albuquerque, New Mexico Attn: Research & Development Col. P. L. Huie Dr. George Young
1	Commander Air Proving Ground Center Eglin Air Force Base Florida Attn: PGTRI
1	Commander Air Force Cambridge Research Center L. G. Hanscom Field Bedford, Massachusetts Attn: Geophysical Research Library
1	Commanding General Field Command Defense Atomic Support Agency P. O. Box 5100 Albuquerque, New Mexico
1	U. S. Atomic Energy Com. Military Applications Div. 1901 Constitution Ave., N. W. Washington 25, D. C.
1	Bureau of Mines, Chief Washington 25, D. C.
1	Commander Air Research Development Command U. S. Air Force Andrews Air Force Base Washington 25, D. C.
1	Deputy Chief of Staff Operations U. S. Air Force Washington 25, D. C. Attn: Asst. for Atomic Energy - AFOAT
1	Johns Hopkins University Operations Research Office 6935 Arlington Road Bethesda 14, Maryland
1	Commanding General U. S. Army Chemical Warfare Laboratories Army Chemical Center, Maryland
1	Commanding Officer Watertown Arsenal Watertown 72, Massachusetts Attn: Laboratory
1	Commanding General Frankford Arsenal Philadelphia 37, Pa. Attn: Pitman-Dunn Lab. Library Branch, C270, Bldg. 40

Distribution List (Cont'd)

No of Copies	Organization
2	Chief of Engineers Department of the Army Washington 25, D. C. Attn: Maj. Maurice K. Kurtz Mr. Martin Kirkpatrick
1	Commanding Officer Picatinny Arsenal Dover, New Jersey Attn: Mr. Joseph Hershkowitz
5	Director Defense Atomic Support Agency Department of Defense Washington 25, D. C. Attn: Mr. John Lewis
1	Director, Army Research Office Arlington Hall Station Arlington, Virginia Attn: Geophysics Branch
1	Executive Secretary Military Liaison Committee to the Atomic Energy Commission 1901 Constitution Avenue, N.W. Washington, D. C.
3	Director Waterways Experiment Station Box 631 Vicksburgh, Mississippi Attn: Mr. G. L. Arbuthnot Mr. William Flathau Mr. Robert Cunny
2	Los Alamos Scientific Laboratory P. O. Box 1663 Los Alamos, New Mexico Attn: Dr. Fred Reines
1	Applied Physics Laboratory Johns Hopkins University 8621 Georgia Avenue Silver Spring, Maryland
1	Armour Research Foundation Illinois Institute of Technology Center Chicago 16, Illinois Attn: Dr. T. H. Schiffman
1	RAND Corporation 1700 Main Street Santa Monica, California Attn: Dr. Brode
1	Sandia Corporation P. O. Box 5800 Albuquerque, New Mexico Attn: Physics Division Mr. W. R. Perret
1	Mr. Kenneth Kaplan Broadview Research Corp. 1811 Trousdale Drive Burlingame, California
1	Professor J. Neils Thompson Civil Engineering Dept. University of Texas Austin 12, Texas
1	Commanding Officer Army Research Office Box CM, Duke Station Durham, North Carolina
1	Stanford Research Institute Menlo Park, California Attn: Mr. F. Sauer
1	Dr. Robert V. Whitman Mass. Institute of Technology Cambridge 39, Massachusetts
1	Dr. Walter Bleakney Princeton University Princeton, New Jersey

Distribution List (Cont'd)

No of Copies	Organization
1	Dr. N. M. Newmark 111 Talbot Laboratory University of Illinois Urbana, Illinois
1	Dr. Otto LaPorte Engineering Research Institute University of Michigan Ann Arbor, Michigan
1	Engineering Research & Development Laboratory Fort Belvoir, Virginia Attn: Dr. T. G. Walsh
1	Dr. Leonard Obert Applied Physics Division U. S. Bureau of Mines College Park 1, Maryland
1	Lawrence Radiation Laboratory Livermore, California Attn: Dr. R. G. Preston
2	Commander Air Force Ballistic Missile Div. Air Force Research & Development Command Washington 25, D. C. Attn: Capt. W. E. Fluhr
1	Director Advanced Research Projects Agency Washington 25, D. C. Attn: Mr. Theodore George
1	Chief of Research & Development Department of the Army Washington 25, D. C. Attn: Lt. Col. Conarty Major Tyler
1	University of New Mexico Albuquerque, New Mexico Att: Mr. Frank Janza KAFB Shock Tube Facility

No of Copies	Organization
1	Professor W. H. Gardner, Jr. College of Engineering Durham, North Carolina
1	V. M. Davis Mine Warfare Branch U. S. Army Engineering Research & Development Lab. Fort Belvoir, Virginia
1	Dr. John M. Davies Pioneering Research Div. Quartermaster Research & Engineering Laboratories Natick, Massachusetts
1	Commanding Officer ASD Wright Patterson A.F.B., Ohio
10	Commanding General U. S. Army Ordnance Aberdeen Proving Ground Aberdeen Proving Ground Maryland Attn: ORDBG-BRU-T Mr. B. Perkins Mr. A. A. Thompson
1	Office of Technical Services Department of Commerce Washington 25, D. C.
1	W. Zagieboylo Quartermaster Research & Engineering Laboratories Natick, Massachusetts
1	Mr. R. C. Bryant Atlantic Research Corp. Shirley Highway at Edsall Rd. Alexandria, Virginia
1	University of Michigan Institute of Science & Tech. Attn: VESIAC, T.W. Caless Box 618 Ann Arbor, Michigan